Thoracoscopic subxiphoid right S^{9+10} segmentectomy: a case report

Dorian Rojas, Bernard Lenot, Karel Pfeuty

Department of Thoracic and Vascular Surgery, Hôpital Yves Le Foll, Saint-Brieuc, France

Correspondence to: Karel Pfeuty, MD. Department of Thoracic and Vascular Surgery, Hôpital Yves Le Foll, Saint-Brieuc 22000, France. Email: karel.pfeuty@armorsante.bzh.

Abstract: Thoracoscopic segmentectomy of posterior (S^{10}) and lateral basal (S^{9}) segments is highly challenging, because of the frequency of anatomical variations and the particularly complex intersegmental plane delimitation, due to the pyramidal shape of the lower lobe. We report here the case of a 77-year-old male presenting with a colorectal metastatic evolutive centimetric nodule deeply located between S^{9} and S^{10} segments, requiring a sub-lobar resection. A thoracoscopic right S^{9+10} segmentectomy was performed through an original subxiphoid approach, combining interlobar fissure and inferior pulmonary ligament approaches and assisted by both three-dimensional computed tomography (3D-CT) anatomical reconstruction and fluorescence imaging. Pathological examination confirmed metastatic nature and complete resection of the nodule with sufficient margin. The patient was integrated in an enhanced recovery after surgery (ERAS) programme and discharge on postoperative day 1 with an uneventful follow-up. Subxiphoid approach appears quite efficient for such complex right S^{9+10} segmentectomy, particularly when designed in a personalized way, based on an accurate anatomical planning strategy for an optimal oncological lung sparing resection.

Keywords: Segmentectomy; subxiphoid; 3D-CT reconstruction; indocyanine green (ICG); case report

Received: 04 August 2021; Accepted: 13 September 2021; Published online: 13 October 2021.

doi: 10.21037/jovs-21-49

View this article at: https://dx.doi.org/10.21037/jovs-21-49

Introduction

Thoracoscopic segmentectomy is a quite appropriate lung-sparing procedure for deep metastasis, ground-glass opacities or early-stage non-small cell lung cancer (NSCLC) in selected patients, with equivalent outcome than lobectomy and well-established functional benefits (1,2).

Among complex segmentectomies, right S^{9+10} segmentectomy is generally considered one of the most challenging (3) and there are several reasons for that: first, the anatomy of those posterior (S^{10}) and lateral (S^{9}) basal segments and their adjacent superior (S^{6}), medial (S^{7}) and anterior (S^{8}) segments, is highly variable; second, the broncho-vascular segmental targets are deeply located within the parenchyma, making their dissection slightly tricky; third, intersegmental plane (ISP) precise delimitation requires a complex three-dimensional stapling approach for extraction of a cuboid S^{9+10} double segment from a pyramidal lower lobe. Thus, preoperative three-dimensional computed tomography (3D-CT) broncho-vascular reconstruction appears nowadays essential and the use of intraoperative techniques for intersegmental plane accurate delimitation, such as fluorescence imaging, is clearly mandatory in order to tackle this complexity.

Historically, two main strategies have been proposed. One is an "interlobar fissure-first" approach involving identification of lower lobe arterial branches before exposure of the hilum of basal segments by creating a posterior tunnel, allowing S^{6} to be partially or totally separated from the basal segments through a posterior or a bidirectional approach (4-6). The other is a single-directional "inferior pulmonary ligament" approach, tracking the target segmental branches, starting with venous distal confluence dissection, followed by bronchial elements before segmental arterial identification, described as the "stem-branch" technique, without the need for interlobar fissure dissection (7-10).

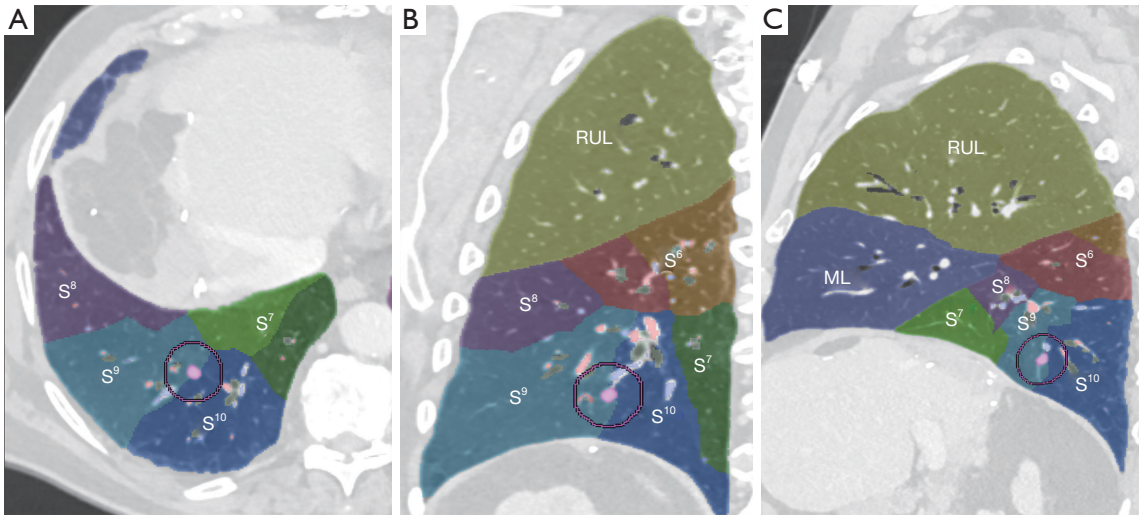

Figure 1 CT multiplanar segmentation (Fujifilm Synapse 3D™). Nodule localization (purple circle) between S^9 and S^{10} after axial (A), coronal (B) and sagittal (C) multiplanar reformation segmentation analysis. RUL, right upper lobe; ML, middle lobe; CT, computed tomography.

We present here a right S^{9+10} segmentectomy through an original bidirectional subxiphoid approach, combining both "interlobar fissure-first" and "inferior pulmonary ligament" approaches associated with a so called "open book" diaphragmatic tunnelling technique between S^{9+10} and S^{7+8} for ISP delimitation. The procedure was assisted by preoperative 3D-CT broncho-vascular reconstruction and intraoperative fluorescence imaging. We present the following article in accordance with the CARE reporting checklist (available at https://jovs.amegroups.com/article/view/10.21037/jovs-21-49/rc).

Case presentation

A 77-year-old man with a metastatic colorectal neoplasia who underwent 2 years before a right hepatectomy for radical metastasis resection, was referred to our department. Chest CT showed 3 lung solid nodules increasing in size up to 1 cm, one deeply located on the right between S^9 and S^{10} and two on the left, one deep seated in S^8 and another more superficial in S^6. Pulmonary functional tests were satisfactory without associated comorbidities and a bilateral lung-sparing strategy was decided after multidisciplinary team concertation. A right S^{9+10} segmentectomy was first planned, before a double left S^8 segmentectomy and S^6 wedge in a second phase, 1 month later.

All procedures performed in this study were in accordance with the ethical standards of the institutional and/or national research committee(s) and with the Helsinki Declaration (as revised in 2013). Written informed consent was obtained from the patient for publication of this case report and accompanying images/video. A copy of the written consent is available for review by the editorial office of this journal.

Anatomical analysis (Figures 1-4)

A personalized preoperative anatomical map was designed on the basis of CT 1 mm slice axial images and 3D-CT reconstruction (Fujifilm Synapse 3D™). Careful analysis of nodule localization was confronted to multiplanar reformation segmentation (*Figure 1*) and positional relationships reconstruction of segmental vessel and bronchi (*Figure 2*) were corelated with basic anatomical landmarks as described by Nomori and Okada (11).

S^{9+10} broncho-vascular anatomical pattern was quite classical with common A^{9+10} and B^{9+10} trunks, whereas the Inferior basal (IBV) vein was found to be a true V^{9+10} without any accessory venous drainage for S^8 or intersegmental plane, with superior basal vein (SBV) receiving V^8 and ISV between S^8 and S^9.

Notably, some relevant anatomical variations (*Figure 3*) were observed on adjacent segments: in particular, superior S^6 presented an atypical lateral S^{6c} sub-segment separated from S^{6a+b}, with A^{6c} and B^{6c} rising distally on basilar bronchial and arterial trunks; also, a protruding medial S^{7b}

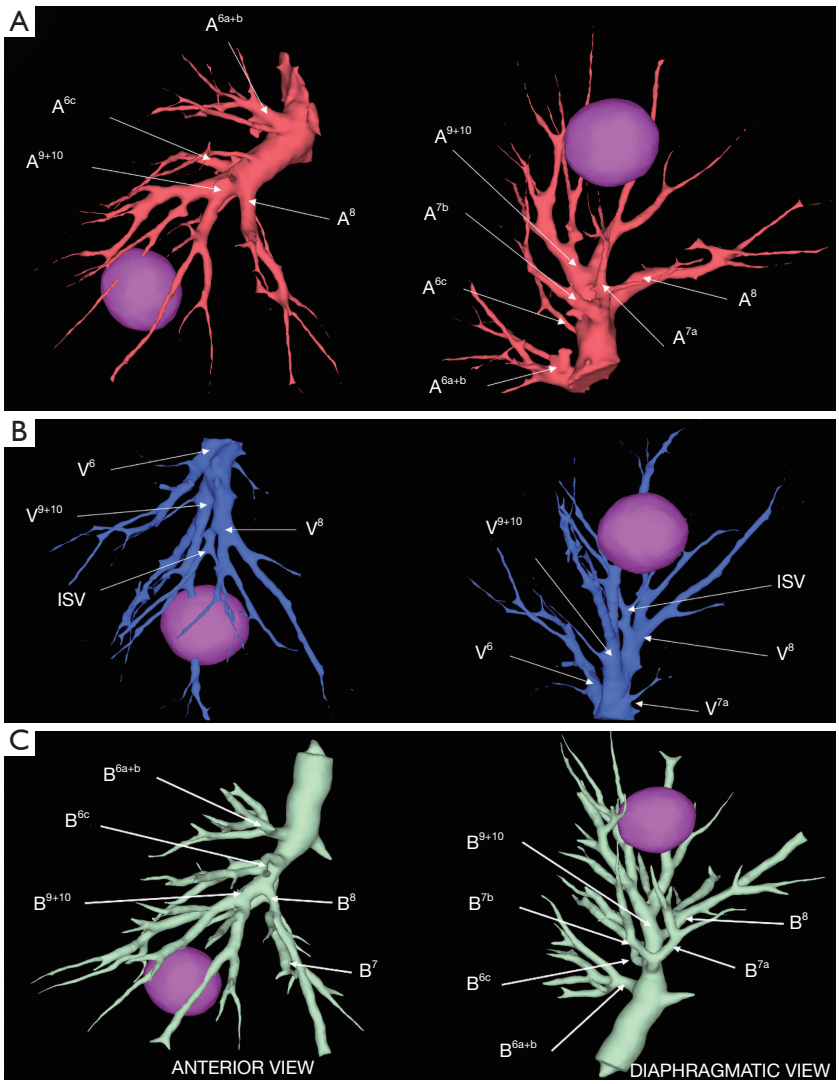

Figure 2 3D-CT bronchial-vascular reconstruction. Anterior and diaphragmatic views of arterial (A), venous (B) and bronchial (C) segmental reconstruction. ISV, intersegmental venous; 3D-CT, three-dimensional computed tomography.

extending over S^{10} was identified, with B^{7b} and A^{7b} running posteriorly between V^{6} and basal vein. This rare variation (14% in frequency) (12) had to be taken in consideration, since S^{7b} subsegment resection was necessary in this case for sufficient margin and to avoid S^{7} congestion, as recommended by Sato and colleagues (5).

In addition, a 3D-CT reconstruction was used for simulation of a 20 mm diameter "halo" around the nodule, that was confronted to the volumetric segmentation in order to anticipate the safety reliable margins for an oncological segmentectomy (*Figure 4*).

Operative techniques (Video 1 and Table 1)

The procedure was performed under thoracoscopic 4K 30° imaging system with immersive 55-inch screen, camera holder stabilization, through a multiportal subxiphoid approach, whose principles have already been described (13). A specific biportal approach has been standardized in our department for all regular right-side resections, with one 4 cm subxiphoid utility port dedicated to dissection, stapling and specimen extraction, and another 1 cm subcostal port on the medio clavicular line used for camera and an

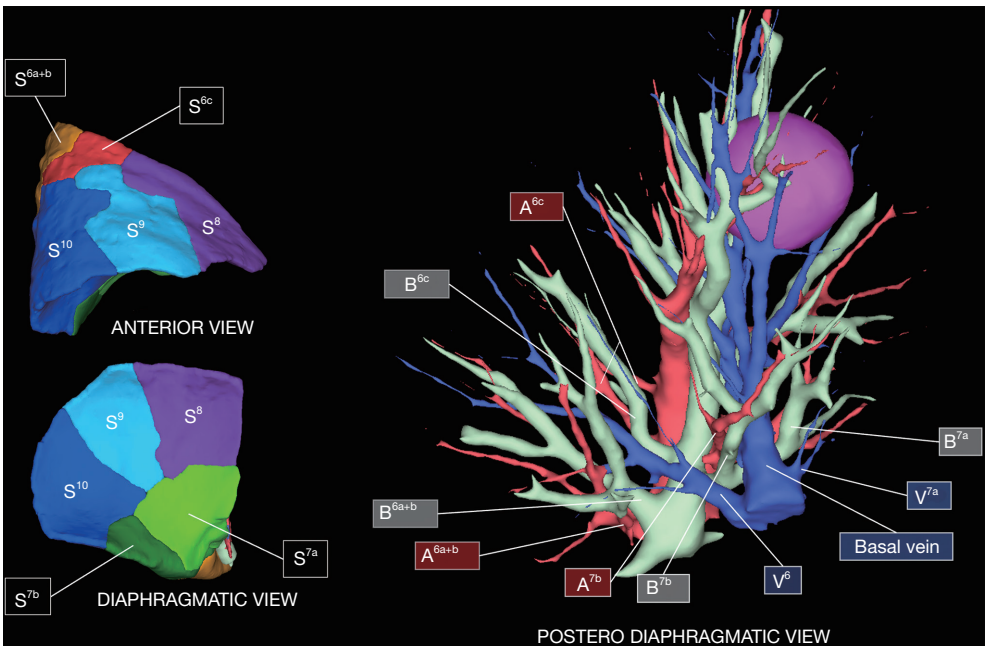

Figure 3 Anatomical variations of adjacent S^7 and S^6. S^6 presented an atypical lateral S^{6c} sub-segment separated from S^{6a+b} with close attention to respect A^{6c} and B^{6c} rising distally on basilar bronchial and arterial trunks. Also, a protruding medial S^{7b} extending over S^{10} was identified, with B^{7b} and A^{7b} running posteriorly between V^6 and basal vein, making S^{7b} additional resection necessary.

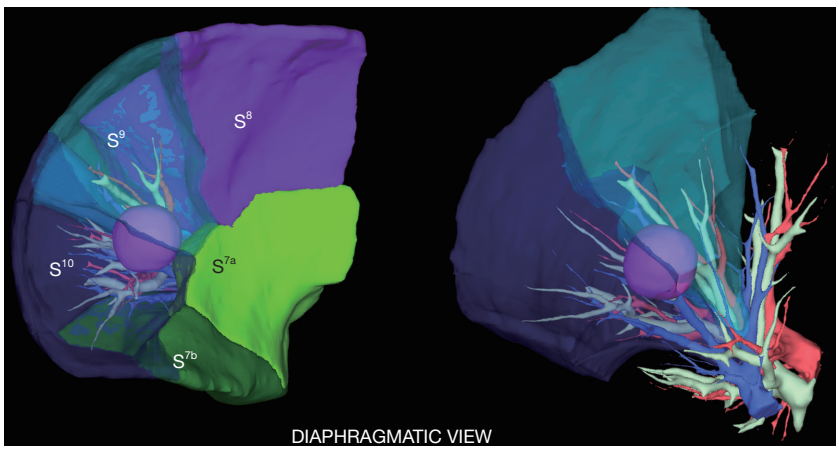

Figure 4 Safety margin halo simulation. A 20 mm diameter "halo" around the nodule was confronted to the volumetric segmentation in order to anticipate safety reliable margins for an oncological segmentectomy.

articulated grasper (*Figure 5*). The surgeons stand both in the front of the patient.

Step 1: anterior interlobar fissure approach

The interlobar pulmonary artery and its branches were first exposed after completing the fissure. Then, A^{9+10} was encircled and stapled after clear identification of adjacent A^8 and A^{6c} arteries. In cases of hypoplastic or incomplete fissure, this approach may be tricky and we usually overcome this by the use of the fissure tunnel technique (14), which prevents postoperative airleak in the same time. This approach is also mandatory in NSCLC indications for an adequate radical hilar lymph node (LN) dissection of stations 10, 11 and 12, with a frozen section

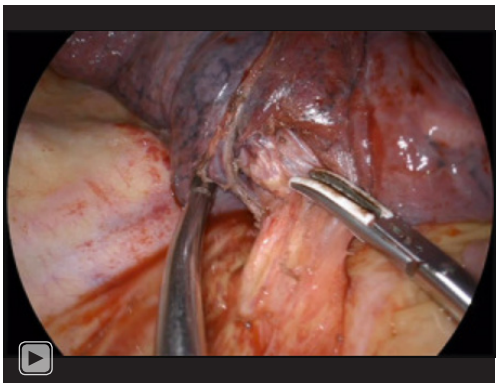

Video 1 This video demonstrates, step by step, a right thoracoscopic S^{9+10} segmentectomy through a subxiphoid approach combining both interlobar fissure and inferior pulmonary ligament approaches, on the basis of 3D-CT reconstruction and fluorescence imaging.

recommended.

Step 2: posterior mediastinal dissection

The patient was then rolled anteriorly and the lower lobe also flipped anteriorly, giving access to subcarinal area for a lobe specific LN dissection of stations 7, 8 and 9, after inferior pulmonary ligament section and sampling of station 11 of the second carina.

Step 3: inferior pulmonary ligament approach

A Trendelenburg patient position was adopted at this step, optimizing the diaphragmatic view. The subxiphoid way gives an interesting panoramic inferior and tangential angle of attack, offering the possibility of an accurate dissection of venous and bronchial segmental branches. IBV was first dissected: small V^{7b} branches were coagulated, V^{7a} was respected and V^{6} and SBV were further identified. As expected, B^{7b} and A^{7b} were recognized running posteriorly between V^{6} and basal vein and B^{7b} was first dissected and stapled. An "open book" approach was then initiated: the principle is to divide S^{9+10} and S^{7+8} following V^{8} "bookmark" from the diaphragmatic side. It started with a first inferior stapling (ISP^{1}) dividing S^{7a} and S^{7b}, respecting V^{7a} and B^{7a} and guided by inferior pulmonary ligament axis. This first division—usually between S^{7} and S^{10} in classical configuration—generally dramatically enhances the access to inferior hilar structures and the deployment of stem-branch technique. IBV was then confirmed to be a true V^{9+10} and was stapled. V^{8} was further deeply dissected

Table 1 Step by step description

Step 1: anterior interlobar fissure approach
Completion of the fissure
Exposure of PA, A^{9+10} and adjacent A^{8} and A^{6c}
Dissection and stapling of A^{9+10}
#11 and #12 node dissection
Step 2: posterior mediastinal dissection
Inferior pulmonary ligament section
Subcarinal lymph node dissection
#11 node dissection
Step 3: inferior pulmonary ligament approach
Dissection and identification of V^{6} and basal segmental veins
Dissection and stapling of B^{7b} between V^{6} and basal vein
Distal dissection of V^{6} and identification of A^{7b}
ISP^{1} diaphragmatic stapling between S^{7b} and S^{7a}
Further dissection of V^{8} "bookmark"
Dissection and clip of V^{9+10}
Dissection and clip of A^{7b}
Dissection of B^{9+10} and identification of adjacent B^{6c} and B^{8}
Step 4: diaphragmatic "open book" basal ISP division
Fluorescence imaging system use after ICG injection (0.3 mg/kg)
ISP delimitation by cauterisation
ISP^{2} and ISP^{3} anterior stapling between S^{8} and S^{9}
Further distal dissection of V^{8} and intersegmental vein "bookmark"
ISP^{4} diaphragmatic tunnel stapling between S^{10} and S^{8}
Dissection and stapling of B^{9+10}
Retrieval of A^{9+10} stump behind B^{9+10} stump
Identification of the fissural tunnel between S^{9+10} and S^{8}
S^{9+10} stump traction rearward
ISP^{5} diaphragmatic tunnel stapling between S^{9} and S^{8}
Step 5: superior and posterior S6 ISP division
Further dissection of V^{6a+b}
ISP^{6} posterior stapling along V6
Identification of A^{6c} and B^{6c}
S^{9+10} stump traction downward
ISP^{7} and ISP^{8} superior and posterior stapling between S^{9+10} and S^{6}

PA, pulmonary artery; ISP, intersegmental plane; ICG, indocyanine green.

inside the hilar structure until intersegmental venous (ISV) branch (between S^8 and S^9) landmark visualization. A^{7b} was then clipped and B^{9+10} and both adjacent B^8 and B^{6c} were identified.

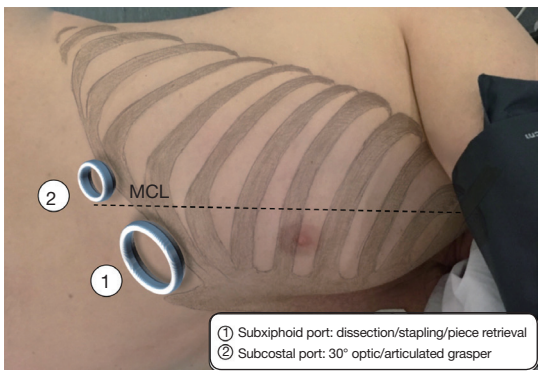

Figure 5 Subxiphoid biportal approach. A paramedian 4 cm subxiphoid port is dedicated to dissection, stapling and piece retrieval, whereas a 1 cm subcostal port on the MCL is used for 30° optic and articulated grasper. MCL, medio clavicular line.

Step 4: "open book" diaphragmatic basal ISP division

Thereafter, a near infra-red fluorescence imaging system (Medtronic Elevision™ IR) was used with single injection of indocyanine green (ICG) at the dose of 0.3 mg/kg, and a demarcation line was clearly obtained and cauterized between S^{9+10} and adjacent still vascularized segments (*Figure 6*). The "open book" technique was deployed peripherally to centrally (*Figure 7*): anterior ISP stapling between S^9 and S^8 was continued (ISP^2 & ISP^3) followed by diaphragmatic tunnel stapling (ISP^4) between S^{10} and S^8, guided by the relevant V^8 landmark. B^{9+10} appeared clearly visible at this step and was stapled. A^{9+10} stump was retrieved behind B^{9+10} stump, which was then pulled up posteriorly. The tunnel reaching previous anterior fissure dissection was identified. S^{9+10} stump traction is very important here in so far as it gives an optimal view for the next ISP diaphragmatic tunnel stapling (ISP^5) dividing S^9 and S^8 centrally, from bottom to top. A small parenchymal bridge was preserved between S^6 and S^8, avoiding any torsion of an isolated S^6.

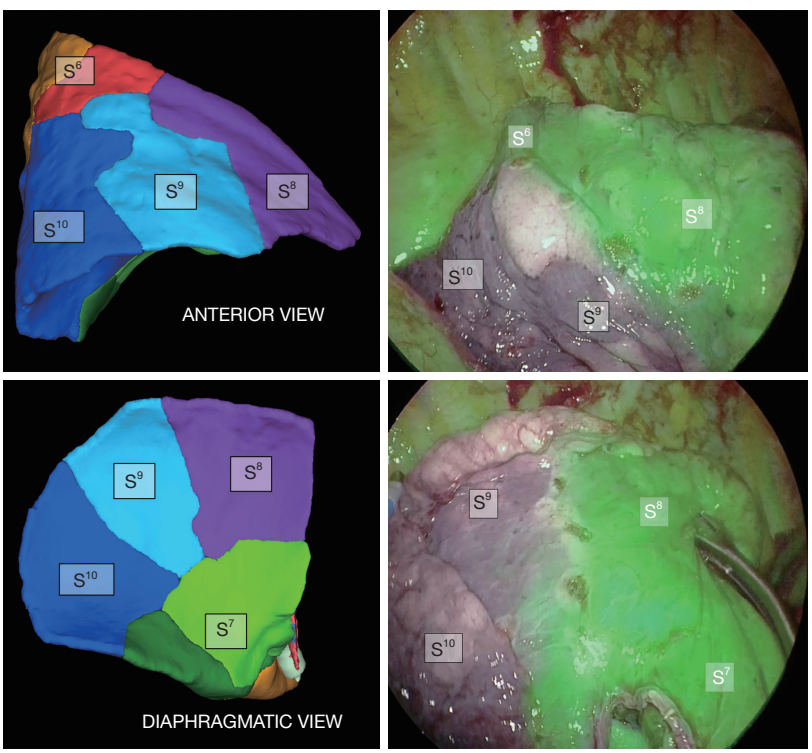

Figure 6 Intersegmental plane fluorescence delimitation (Medtronic Elevision™ IR). After A^{9+10} stapling, A single intravenous injection of green indocyanine (0.3 mg/kg) allowed an accurate delimitation of intersegmental plane, with a high degree of precision when compared to 3D-CT reconstruction. 3D-CT, three-dimensional computed tomography.

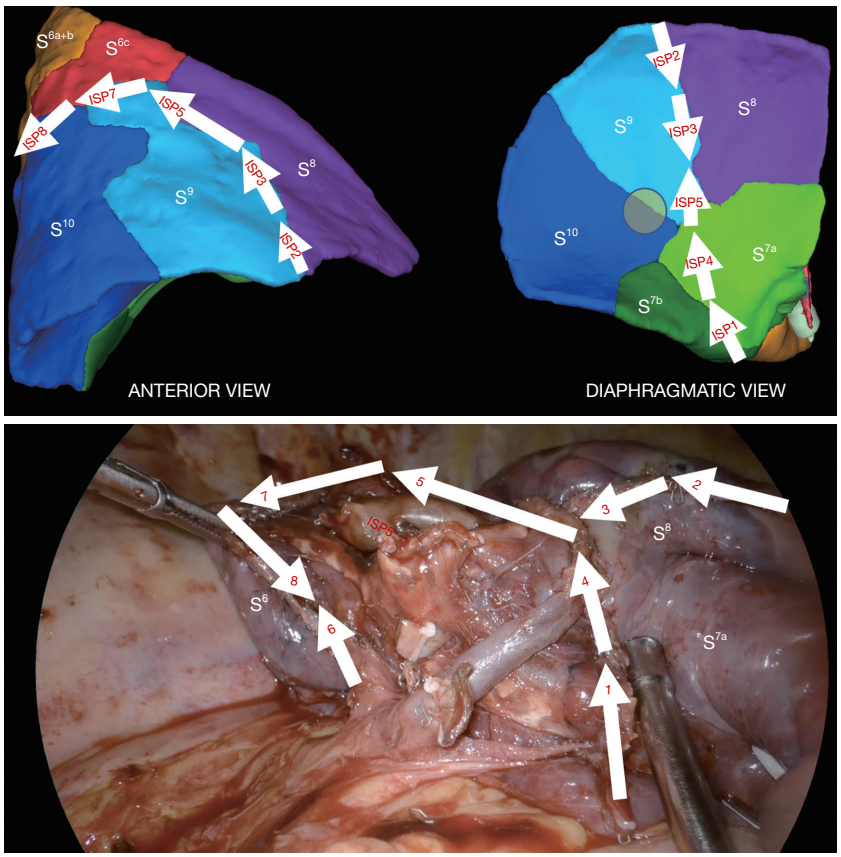

Figure 7 Intersegmental plane stapling steps. ISP stapling was conducted from diaphragmatic side bottom up following V8/Intersegmental vein landmark and fluorescence demarcation line, beginning with Basal "open book" split from S^{8+7a}, followed by postero-superior division with S^6. ISP, intersegmental plane.

Step 5: posterior and superior S6 ISP division

The posterior and superior ISP division was finally completed between S^{9+10} and S^6, guided by V^6 posteriorly (ISP^6) and by fluorescence demarcation line superiorly (ISP^7 and ISP^8) with a particular attention paid to A6c and B6c rising unusually distally in this case. S^{9+10} stump traction downward is quite helpful during this step.

Step 6: pathological examination

The piece was extracted through the subxiphoid port and metastatic nature of the nodule was confirmed on frozen section, with a sufficient 2 cm safety margin.

Step 7: final anatomical view

The final anatomical and ISP views were checked (*Figures 7,8*) and satisfying reventilation of remaining segments was also confirmed without airleak. A 24 Fr subxiphoid chest tube was then placed.

Postoperative course

The patient was extubated in operating room and integrated in an enhanced recovery after surgery (ERAS) programme associating early physiotherapy, feeding and mobilization and opioid-free analgesia limited to a combination of non-steroid anti-inflammatory drugs and paracetamol. He was discharged on postoperative day-1 after early chest tube removal (15) with an uneventful postoperative course. The final pathological examination confirmed complete resection of a 10 mm metastatic nodule with 2 cm margin free and 12 negative nodes. A double left S^8 segmentectomy and S^6 wedge was planned one month later after CT control, showing a quite satisfying ventilation of remaining adjacent segments (*Figure 9*).

Discussion

Thoracoscopic anatomical segmentectomy is actually a

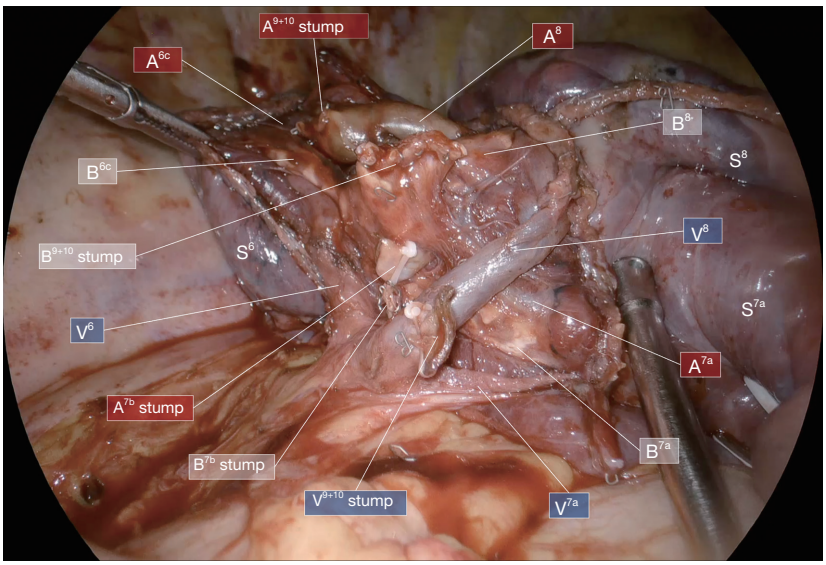

Figure 8 Final anatomical view.

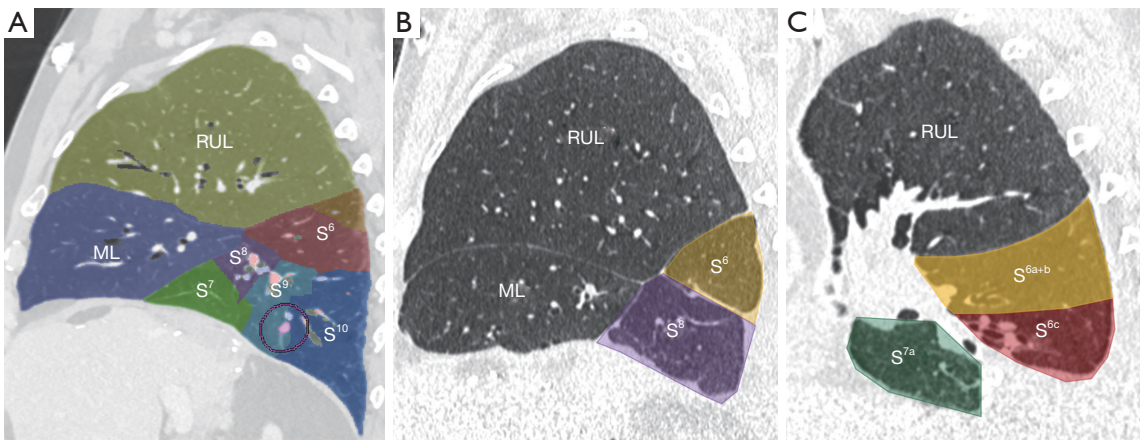

Figure 9 CT anatomical result. CT control showed satisfying ventilation of remaining adjacent segments on sagittal view, one month after surgery. (A) Before surgery; (B,C) 1 month after surgery. The purple circle in (A) indicates nodule localization. RUL, right upper lobe; ML, middle lobe; CT, computed tomography.

standard of care for surgical treatment of deep metastasis and ground glass opacities and is taking an increasingly important place in the area of early-stage NSCLC treatment, that could be soon reinforced by the expected long-term results of the major ongoing JCOG-0802 study on the topics (16). If we add this to the trend in emergence of efficient lung cancer screening programs (17), thoracic surgeons will certainly have to deal in the near future with a wide and growing range of complex segmentectomy of which right S^{9+10} segmentectomy is probably one of the most challenging.

Three main issues can be highlighted to explain this complexity, one around the high frequency of anatomical variation, another concerning the deep-seated location of broncho-vascular segmental targets and last but not least the multi-directional three-dimensional stapled-based delimitation of intersegmental plane. Overcoming these 3 key points requires above all an overall personalized planning strategy, involving imperative anatomical preoperative 3D-CT planning for an accurate anatomical

knowledge, preoperative technical planning for an appropriate tracking of broncho-vascular segmental elements and again preoperative planning of ISP delimitation for which fluorescence imaging is becoming the technique of choice.

We described herein an original subxiphoid approach for achieving such complex segmentectomy, combining both interlobar fissure and inferior pulmonary ligament approaches. Although still little used, subxiphoid approach has already proven to be feasible, safe and efficient for simple as well as complex segmentectomies in experienced centers (18) and presents some advantages: it's a highly minimally invasive painless approach offering a great synergy with ERAS programmes and giving a particularly interesting view for basal segmentectomies. The standardized subxiphoid biportal approach, which was developed in our department for right-side resection (14), supports this statement: the duplicated subcostal panoramic view allows to deal with the same vision quality whether for interlobar fissure or inferior pulmonary ligament step, while leaving a great ease of movement and dissection accuracy through the subxiphoid port. This approach is also very interesting for deployment of tunnel techniques from anterior to posterior on fissural side in cases of hypoplastic fissure (15) as from bottom to top on diaphragmatic side for ISP delimitation.

When focusing on technical points, some authors recommend to start with interlobar fissure arterial dissection with a view to initiate the posterior tunnel giving the way of ISP between S6 and basal segments (4-6). We emphasize here that early A^{9+10} stapling during this first interlobar step is greatly helpful to take the better benefit of further fluorescence imaging and that splitting S^{6} can be delayed at the last step after the "open book" basal splitting of $^{S9+10}$ from S^{7+8}. Anterior fissure dissection also gives an easier access to hilar and segmental LN dissection, a mandatory step in NSCLC indications. Furthermore, it facilitates for us the following Inferior pulmonary ligament approach, described by its defenders as a "stem branch technique" contributing to an easier reliable tracking of deeply located targeted segmental branches, successively, venous, bronchial, and then arterial one (7-10). This unidirectional inferior approach avoids also unnecessary fissure dissection and airleaks that goes with it but is not totally satisfactory in an oncological perspective. We decided then to associate the advantages of both approaches through this original bidirectional subxiphoid way.

ISP management also remains a major issue: bronchial inflation method was historically the first used. It is now regarded as too approximate due to the frequency of residual parenchymal bridges between segments, particularly in patients with lung obstructive disorder, compared to fluorescence imaging, which is nowadays the technique of choice by its accuracy to distinguish targeted segments from adjacent still vascularized ones (19,20). Other techniques have been proposed, like slip knot method (21), endobronchial dye injection (22) and Oizumi and colleagues still consider extensive venous dissection of intersegmental veins as an important landmark for an adequate ISP delimitation (23). De facto, our "open book" diaphragmatic approach illustrates in this case the effective combination of both fluorescence imaging and ISV extensive dissection: basal ISP stapling was deployed peripherally to centrally from diaphragmatic side first, following ICG marking and V8/ISV "bookmark" before completing S6 ISP. We have to highlight here the great subxiphoid view provided for crucial S^{9+10} stump traction downward and rearward during this phase.

Lastly, regarding S^{7} adjacent segment management, described by Sato and colleagues as an often-neglected step (5), subxiphoid approach was very appropriate in conjunction with preoperative 3D-CT reconstruction, to avoid any misidentification of the S^{7b} anatomical variation encountered in this case.

Conclusions

Subxiphoid approach is an effective alternative approach for such complex right S^{9+10} anatomical segmentectomy. Beyond the surgical approach chosen, complex thoracoscopic segmentectomy has nowadays to be tackled via an overall personalized planning strategy, assisted by 3D-CT anatomical reconstruction and intersegmental plane accurate delimitation techniques as fluorescence imaging and integrated in ERAS dynamics, for an optimal oncological lung-sparing sub-lobar resection.

Acknowledgments

Funding: None.

Footnote

Provenance and Peer Review: This article was commissioned by the Guest Editor (Michel Gonzalez) for the series "VATS Segmentectomy" published in *Journal of Visualized Surgery*. The article has undergone external peer review.

Reporting Checklist: The authors have completed the CARE reporting checklist. Available at https://jovs.amegroups.com/article/view/10.21037/jovs-21-49/rc

Peer Review File: Available at https://jovs.amegroups.com/article/view/10.21037/jovs-21-49/prf

Conflicts of Interest: All authors have completed the ICMJE uniform disclosure form (available at https://jovs.amegroups.com/article/view/10.21037/jovs-21-49/coif). The series "VATS Segmentectomy" was commissioned by the editorial office without any funding or sponsorship. KP declares as educational webinar lecturer for MEDTRONIC. The authors have no other conflicts of interest to declare.

Ethical Statement: The authors are accountable for all aspects of the work in ensuring that questions related to the accuracy or integrity of any part of the work are appropriately investigated and resolved. All procedures performed in this study were in accordance with the ethical standards of the institutional and/or national research committee(s) and with the Helsinki Declaration (as revised in 2013). Written informed consent was obtained from the patient for publication of this case report and accompanying images/video. A copy of the written consent is available for review by the editorial office of this journal.

References

1. Handa Y, Tsutani Y, Mimae T, et al. Surgical Procedure Selection for Stage I Lung Cancer: Complex Segmentectomy versus Wedge Resection. Clin Lung Cancer 2021;22:e224-33.
2. Bédat B, Abdelnour-Berchtold E, Krueger T, et al. Impact of complex segmentectomies by video-assisted thoracic surgery on peri-operative outcomes. J Thorac Dis 2019;11:4109-18.
3. Handa Y, Tsutani Y, Mimae T, et al. Complex segmentectomy in the treatment of stage IA non-small-cell lung cancer. Eur J Cardiothorac Surg 2020;57:114-21.
4. Igai H, Kamiyoshihara M, Kawatani N, et al. Thoracoscopic lateral and posterior basal (S9+10) segmentectomy using intersegmental tunnelling. Eur J Cardiothorac Surg 2017;51:790-1.
5. Sato M, Murayama T, Nakajima J. Thoracoscopic stapler-based "bidirectional" segmentectomy for posterior basal segment (S10) and its variants. J Thorac Dis 2018;10:S1179-86.
6. Gossot D, Seguin-Givelet A. Thoracoscopic right S9+10 segmentectomy. J Vis Surg. Sept 2018;4:181.
7. Kikkawa T, Kanzaki M, Isaka T, et al. Complete thoracoscopic S9 or S10 segmentectomy through a pulmonary ligament approach. J Thorac Cardiovasc Surg 2015;149:937-9.
8. Oizumi H, Kato H, Suzuki J, et al. Thoracoscopic anatomical S10 segmentectomy: a posterior approach. J Vis Surg 2018;4:142.
9. Zhu Y, Pu Q, Liu L. Trans-inferior-pulmonary-ligament VATS basal segmentectomy: application of single-direction strategy in segmentectomy of left S9+10. J Thorac Dis 2018;10:6266-8.
10. Liu C, Liao H, Guo C, et al. Single-direction thoracoscopic basal segmentectomy. J Thorac Cardiovasc Surg 2020;160:1586-94.
11. Nomori H, Okada M. Illustrated anatomical segmentectomy for lung cancer. Springer, 2012:92-113.
12. Shimizu K, Nagashima T, Yajima T, et al. Thoracoscopic Medial-Basal Segment Segmentectomy. Ann Thorac Surg 2017;104:e403-6.
13. Pfeuty K, Lenot B. Multiportal subxiphoid thoracoscopic major pulmonary resections. J Thorac Dis 2019;11:2778-87.
14. Decaluwe H, Sokolow Y, Deryck F, et al. Thoracoscopic tunnel technique for anatomical lung resections: a 'fissure first, hilum last' approach with staplers in the fissureless patient. Interact Cardiovasc Thorac Surg 2015;21:2-7.
15. Pfeuty K, Lenot B. Early postoperative day 0 chest tube removal using a digital drainage device protocol after thoracoscopic major pulmonary resection. Interact Cardiovasc Thorac Surg 2020;31:657-63.
16. Suzuki K, Saji H, Aokage K, et al. Comparison of pulmonary segmentectomy and lobectomy: Safety results of a randomized trial. J Thorac Cardiovasc Surg 2019;158:895-907.
17. de Koning HJ, van der Aalst CM, de Jong PA, et al. Reduced Lung-Cancer Mortality with Volume CT Screening in a Randomized Trial. N Engl J Med

2020;382:503-13.
18. Ali J, Haiyang F, Aresu G, et al. Uniportal Subxiphoid Video-Assisted Thoracoscopic Anatomical Segmentectomy: Technique and Results. Ann Thorac Surg 2018;106:1519-24.
19. Yotsukura M, Okubo Y, Yoshida Y, et al. Indocyanine green imaging for pulmonary segmentectomy. JTCVS Tech 2021;6:151-8.
20. Guigard S, Triponez F, Bédat B, et al. Usefulness of near-infrared angiography for identifying the intersegmental plane and vascular supply during video-assisted thoracoscopic segmentectomy. Interact Cardiovasc Thorac Surg 2017;25:703-9.
21. Oizumi H, Kato H, Endoh M, et al. Slip knot bronchial ligation method for thoracoscopic lung segmentectomy. Ann Thorac Surg 2014;97:1456-8.
22. Sato M, Omasa M, Chen F, et al. Use of virtual assisted lung mapping (VAL-MAP), a bronchoscopic multispot dye-marking technique using virtual images, for precise navigation of thoracoscopic sublobar lung resection. J Thorac Cardiovasc Surg 2014;147:1813-9.
23. Oizumi H, Kanauchi N, Kato H, et al. Anatomic thoracoscopic pulmonary segmentectomy under 3-dimensional multidetector computed tomography simulation: a report of 52 consecutive cases. J Thorac Cardiovasc Surg 2011;141:678-82.

doi: 10.21037/jovs-21-49
Cite this article as: Rojas D, Lenot B, Pfeuty K. Thoracoscopic subxiphoid right S^{9+10} segmentectomy: a case report. J Vis Surg 2023;9:19.